2020-07-10

CAPE VERDE BEACH HAZARDS

Stokes, C

http://hdl.handle.net/10026.1/16918

CAPE VERDE BEACH HAZARDS

Report provided by: Coastal Marine Applied Research,

University of Plymouth Enterprise Ltd.

Report provided for: Adam Wooler

Date: 10/07/2020

Project code: 1710

Document code/version: 1710_v1

CMAR: Coastal Marine Applied Research

CMAR is a research-informed consultancy group based in the School of Biological and Marine Sciences at the University of Plymouth, south west UK, and contract our services through the university's wholly owned commercial subsidiary, University of Plymouth Enterprise Limited (UoPEL). We focus on coastal processes and marine physics, and aim to provide a first-class data collection, analysis, modelling, and synthesis service to help address important issues in the coastal and marine environment. We strive to understand and predict the behaviour of coastal, marine and estuarine systems to support the appropriate management of resources and activities in these environments. Our team consists of highly qualified coastal scientists and engineers, and our research on coastal dynamics is published in international, peer-reviewed journals.

All queries related to this document should be directed to:

CMAR, School of Biological and Marine Sciences, Reynolds Building, University of Plymouth, Drake Circus, Plymouth, Devon PL4 8AA

Email: cmar@plymouth.ac.uk

Telephone: +44 1752 586177

Web: www.plymouth.ac.uk/cmar

Twitter: @pu_cmar

UNIVERSITY OF PLYMOUTH | Coastal Marine Applied Research

Document Information

Document permissions	Adam Wooler
Project number	1710
Project name	CAPE VERDE BEACH HAZARDS
Report date	10th July 2020
Report number	1710_v1
Client	Adam Wooler
Client representative	Adam Wooler
Project lead	Dr Christopher Stokes
Project manager	Dr Tim Scott

Document history

Date	Issue	Prepared	Approved	Authorised	notes
06/07/20	Draft	CS	TS	GM	
08/07/20	Revised draft	CS	TS	GM	

Document authorisation

Prepared	Approved	Authorised
Dr Christopher Stokes	Dr Tim Scott	Prof. Gerd Masselink

Deliverable Title

Executive Summary

Coastal Marine Applied Research (CMAR) have been commissioned by Adam Wooler to assess physical bathing hazards at Praia de Lacacao, Boa Vista, Cape Verde. A number of bathing injuries have occurred at the beach adjacent to the RIU Touareg Hotel, and this report seeks to estimate the wave and beach morphology conditions at the times of the bathing incidents, as well as to identify typical bathing conditions that occur throughout the year at the beach.

Through a process of expert judgement using a combination of wave analysis, and assessment of in-situ and satellite imagery, the beach at Praia de Lacacao is expected to be consistently at the 'reflective' end of the beach morphology spectrum. The likely beach profile gradient in the area of wave breaking is expected to be consistently within the range 0.1 – 0.2 (slope of 1-in-10 to 1-in-5), which represents a steep beach profile. Steep beaches exposed to small wave heights with long wavelengths experience plunging or surging/collapsing wave breakers, which break intensely over a short part of the beach profile, or dissipate their energy entirely at the shoreline. Given the expected beach morphology and wave breaker types, shore-break impact injuries are expected to be the primary beach hazard type at Praia de Lacacao.

From processed wave model data, breaking wave heights at the site are predicted to vary from 0.5 – 3 m, but only exceed 1.7 m 10% of the time. Wave conditions do not vary significantly throughout the year, and average summer and winter breaking wave heights vary from 0.9 – 1.0 m, with peak wave periods of 10.2 – 11.0 s. Wave breaking is predicted to be consistently within the 'plunging' to 'surging/collapsing' regimes. In-situ photographs of waves breaking at Praia de Lacacao confirm that waves typically break very close to the beach, and under larger waves (breaking wave height, $H_b > 1$ m) break as plunging breakers with considerable breaking intensity and power at the shoreline.

During five of the six bathing incidents, the wave conditions are predicted to have been below the average breaking wave height for the season in which they occurred, ranging from $H_b = 0.6$ m – 0.9 m. During one of the six incidents, the wave conditions are predicted to have been $H_b = 2$ m – a wave height which is above average for the season and is exceeded less than 10% of the time at Praia de Lacacao. During all of the incidents, plunging to surging/collapsing breakers are predicted to have been occurring on the beach.

Contents

1. Introduction 1

2. Site Morphology and physical hazards 4

3. Site Wave Climate 9

4. Conditions at the times of the bathing incidents 20

5. Conclusions 22

References 23

Appendix A. Expertise of the CMAR team 24

Appendix B. Processing of wave model data 27

Appendix C. Wave conditions for each incident 28

Table of Figures

Figure 1. Praia de Lacacao beach and RIU Touareg Hotel, Boa Vista, Cape Verde. 1

Figure 2. Location maps showing Cape Verde off the west African coast (upper left), Boa Vista island in the centre of Cape Verde (upper right), and Praia de Lacacao beach and RIU Touareg Hotel on the southern side of Boa Vista island (lower). 2

Figure 3. Chart of bathymetric depth in the Cape Verde island chain, from the General Bathymetric Chart of the Oceans (GEBCO) database (https://www.gebco.net/). Praia de Lacacao on the island of Boa Vista is demarked with a red star. Note that the coastal shelf visible around Boa Vista Island is less than 100 m depth. 3

Figure 4. Beach morphology types for microtidal beaches, identified by Wright and Short (1984). The red box indicates the most likely beach morphology type to occur at Praia de Lacacao, Boa Vista, Cape Verde. 6

Figure 5. Sentinel-2 satellite imagery of Praia de Lacacao, Boa Vista, Cape Verde showing (from top to bottom) low to high energy wave conditions, respectively, and the full range of surf-zone width (visible as a band of white-water) from the 275 images between June 2016 and June 2020. Panel A shows typical surf-zone width, while panel D shows the widest surf-zone, which occurred only once in the images. 7

Figure 6. Aerial imagery of Praia de Lacacao, showing beach cusp formations at the shoreline. 8

Figure 7. Photograph of beach sediment at Praia de Lacacao, extracted from a tourist photograph posted on Google Maps. 8

Figure 8. Upper panel: Wave model output location at 15.9° latitude, -22.9° longitude, approximately 21.5 km directly offshore of Praia de Lacacao, in deep water (>1000 m depth). Lower panels: wave roses showing proportion of wave heights (lower left) and wave periods (lower right) from different directional sectors at the wave model output location. 11

Figure 9. Cross-sectional representation of the three main types of breaking waves: spilling, plunging, surging (or collapsing). 12

Figure 10. Wave hindcast time series from the WAVERYS global wave model, output in deep water approximately 21.5 km offshore of Praia de Lacacao. Vertical dashed lines show the dates on which the beach incidents occurred. The horizontal dashed lines in the lower panel show the thresholds that differentiate between spilling, plunging, and surging/collapsing breakers. The blue and red lines in the lower panel show the upper and lower estimate of the Iribarren Number, based on the upper and lower estimates of beach slope. Black lines in each panel show a monthly moving average (only shown for H_b in top panel for clarity). 14

Figure 11. Wave hindcast time series from the WAVERYS global wave model, output in deep water approximately 21.5 km offshore of Praia de Lacacao, for the year 2012. Vertical dashed lines show the

dates on which the beach incidents occurred. The horizontal dashed lines in the lower panel show the thresholds that differentiate between spilling, plunging, and surging/collapsing breakers. The blue and red lines in the lower panel show the upper and lower estimate of the Iribarren Number, based on the upper and lower estimates of beach slope. 15

Figure 12. Examples of wave breaking at Praia de Lacacao under 'low wave energy' conditions (estimated as $0 < H_b < 0.5$ m). 17

Figure 13. Examples of wave breaking at Praia de Lacacao under 'medium wave energy' conditions (estimated as $0.5 < H_b < 1$ m). 18

Figure 14. Examples of wave breaking at Praia de Lacacao under 'upper wave energy' conditions (estimated as H_b >1 m). 19

Figure 15. Wave conditions for a week either side of incident number 1 (18th April 2012). 28

Figure 16. Wave conditions for a week either side of incident number 2 (16th May 2012). 29

Figure 17. Wave conditions for a week either side of incident number 3 and 4 (15th and 16th of September 2012). 30

Figure 18. Wave conditions for a week either side of incident number 5 (8th October 2012). 31

Figure 19. Wave conditions for a week either side of incident number 6 (4th November 2012). 32

1. Introduction

Coastal Marine Applied Research (CMAR) have been commissioned by Adam Wooler to assess physical bathing hazards at Praia de Lacacao (Figure 1), Boa Vista, Cape Verde. A number of bathing injuries (herein also referred to as 'the bathing incidents') have occurred at the beach adjacent to the RIU Touareg Hotel (herein also referred to as 'the hotel'), and this report seeks to estimate the wave and beach morphology conditions at the times of the bathing incidents, as well as to identify typical bathing conditions that occur throughout the year at the beach. Praia de Lacacao (herein also referred to as 'the beach') is situated on the southern side of Boa Vista, in the Cape Verde islands, off the western coast of Africa in the Atlantic Ocean. The hotel is situated at a latitude approximately 16°N and longitude of 22.8°W. The beach consists of approximately 7.7 km of uninterrupted beach frontage, and at the location of the RIU Touareg Hotel, the beach faces an orientation of 185° from North (Figure 2). The beach has a small 'microtidal' tide range of 1 m at spring tides (From Admiralty Total Tide data). There is a relatively shallow coastal shelf (< 100 m depth) surrounding the island of Boa Vista (Figure 3).

Figure 1. Praia de Lacacao beach and RIU Touareg Hotel, Boa Vista, Cape Verde.

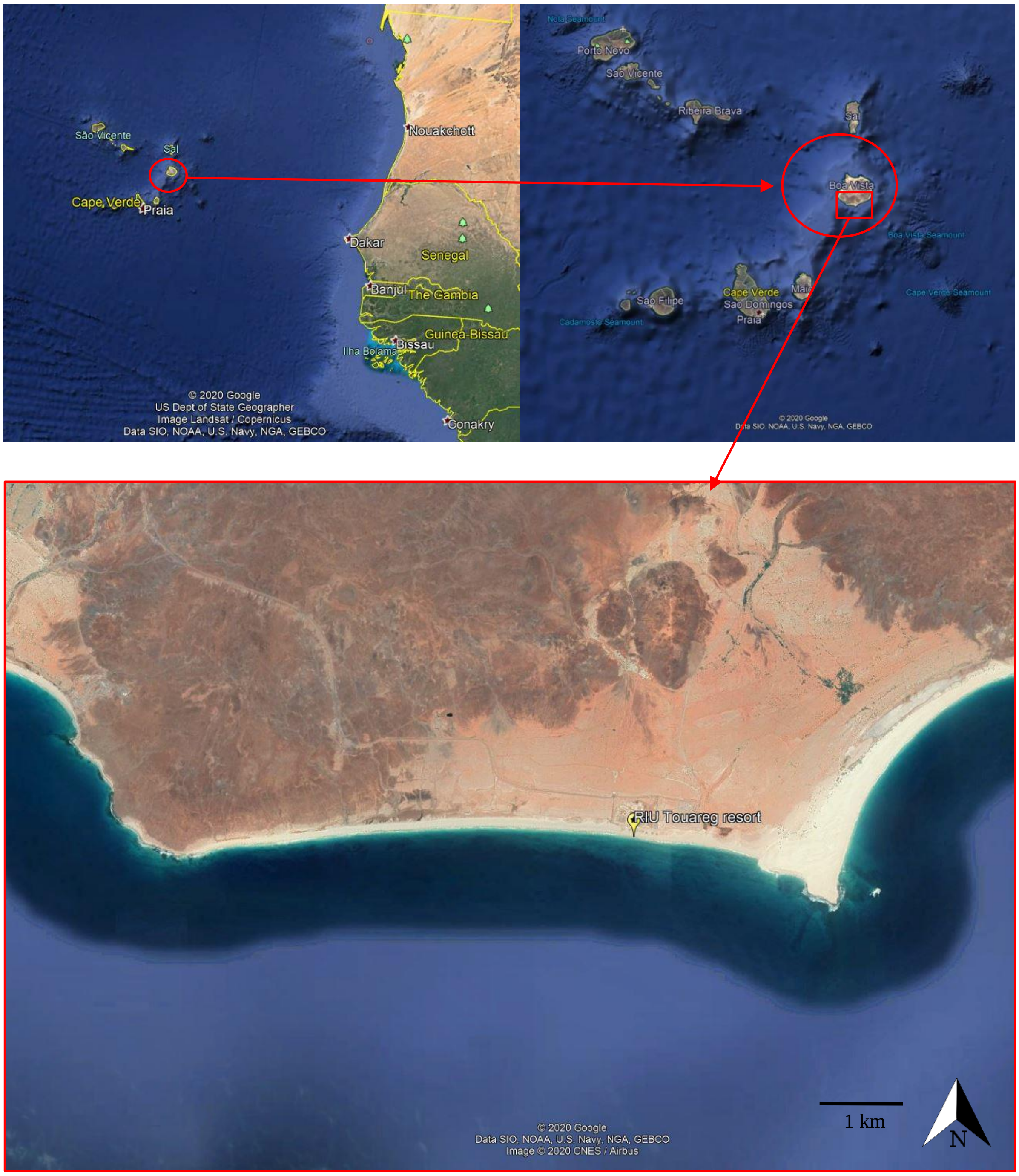

Figure 2. Location maps showing Cape Verde off the west African coast (upper left), Boa Vista island in the centre of Cape Verde (upper right), and Praia de Lacacao beach and RIU Touareg Hotel on the southern side of Boa Vista island (lower).

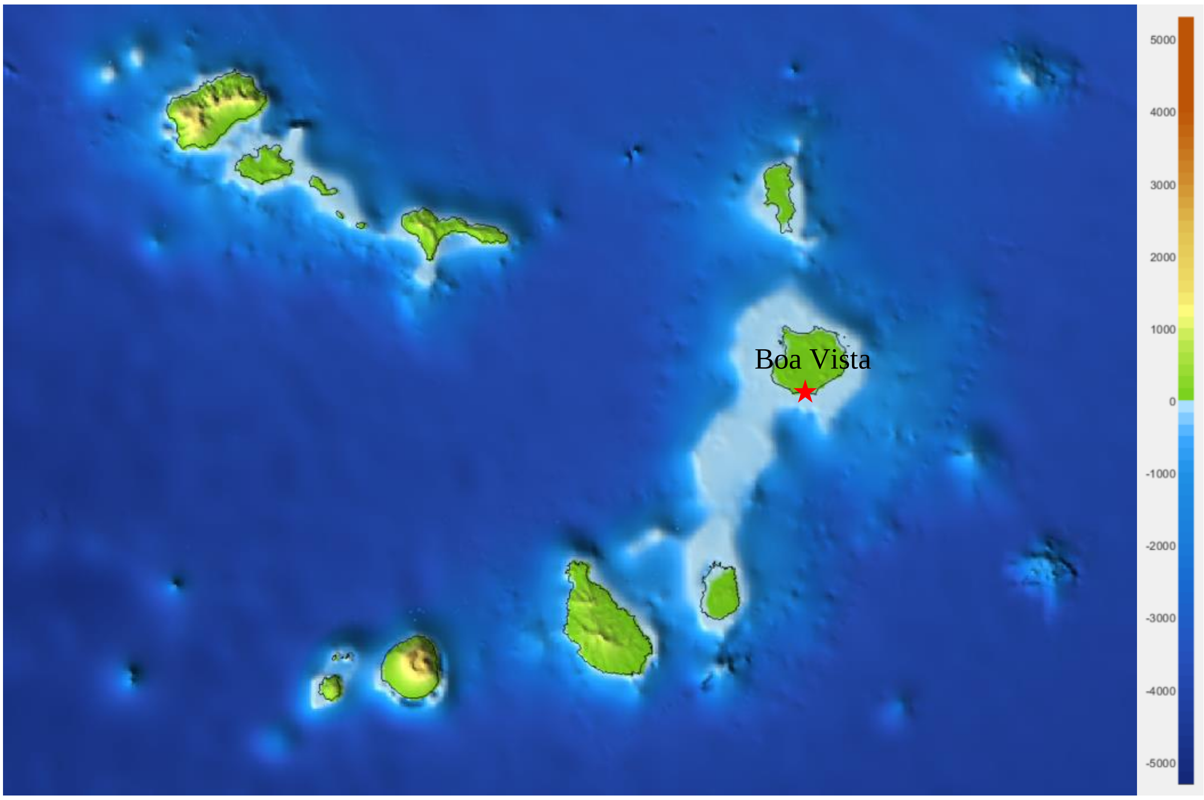

Figure 3. Chart of bathymetric depth in the Cape Verde island chain, from the General Bathymetric Chart of the Oceans (GEBCO) database (https://www.gebco.net/). Praia de Lacacao on the island of Boa Vista is demarked with a red star. Note that the coastal shelf visible around Boa Vista Island is less than 100 m depth.

2. Site Morphology and physical hazards

Beach morphology is a key driver of physical beach hazards, and the planform and profile shape of a beach determines to a large degree which physical hazards are likely to be encountered. The two primary causes of surf zone injuries and drownings worldwide are rip currents and shore-break waves (Castelle *et al.*, 2019). Rip currents are dangerous flows that can take bathers from the shallows out to sea and cause hundreds of drownings and tens of thousands of beach rescues (~70%) globally each year (Castelle *et al.*, 2016), while shore-break waves feature concentrated and intense breaking of waves at the shoreline and tend to cause impact injuries such as bone fractures and spinal injuries, but make up a smaller proportion of surf-zone injuries globally (Castelle *et al.*, 2019). While rip currents are found predominantly on beaches in the 'intermediate' beach morphology range (Figure 4) and are typically driven by bathymetric channels in the beach face, shore-break waves typically occur on steep beach profiles, and therefore most often occur on 'reflective' beach types (Figure 4) or on the steep upper (high-tide) part of the profile of intermediate beach types.

Beach topographic/bathymetric survey data (for example measured profiles) were not available for this analysis, so it is impossible to be certain about the beach profile and gradient at the beach, especially at the times of each individual incident. Instead, the beach morphology at Praia de Lacacao was assessed through a process of expert judgement using a combination of wave analysis (Section 3), and assessment of in-situ imagery (from Google Maps photographs) and satellite imagery (from the Sentinel-2 satellite, covering June 2016 – June 2020). From this analysis, it was concluded that **the beach at Praia de Lacacao is consistently at the 'reflective' end of the beach morphology spectrum** (see Figure 4 for beach morphology types)**.** This was determined from the following evidence:

- The satellite imagery shows a consistently narrow surf-zone (Figure 5), void of visible rip currents or channels. The surf-zone is on the order of 0 - 20 m wide for approximately 90% of the 275 available Sentinel-2 images, and only exceeded 100 m width once during extreme wave conditions. This is a clear indication of a steep reflective beach type, as shallow beach profiles consistently exhibit wide surf-zones, on the order of 100s of meters wide, even during modest wave conditions.
- Active beach cusps are always visible in the 15 available Google Earth aerial images between March 2005 and October 2019 (Figure 6), and are features that are exclusively found on steep beaches in the upper intermediate to reflective morphology range (i.e. panels e-f, Figure 4).
- Tourist photographs of the beach indicate the sediment is likely to consist of 'medium sand' (for example, Figure 7) with a grain size on the order of 0.25 – 0.5 mm diameter.

- Dimensionless fall velocity, Ω, is a parameter often used to estimate beach morphological state (Wright and Short, 1984; Masselink and Short, 1993). This can be computed from the average breaking wave height (H_b = 1.2 m, from Section 3), the average wave period (T = 8.1 s, from Section 3), and using the estimated range of sediment diameter (0.25 – 0.5 mm) to estimate the sediment fall velocity (ω_s = 0.25 – 0.5 cm/s, following Fig. 1 of Dean (1991)), as $\Omega = H_b/\omega_s T$. This yields average values for Ω of 0.3 – 0.6, which is well within the reflective beach state range of $0<\Omega<1$ (Wright and Short, 1984; Masselink and Short, 1993).

The beach profile gradient is an important consideration in this report, as this parameter strongly influences the intensity of wave breaking at the shore and is used to assess the variability in breaker types in Sections 3 and 4 of the report. Reflective beach morphology typically has a steep profile gradient on the order of 0.1 – 0.2 at the shoreline (Wright and Short, 1984; Masselink and Short, 1993), as depicted Figure 4. Therefore, we consider **the likely beach profile gradient in the area of wave breaking at Praia de Lacacao to be consistently within the range 0.1 – 0.2 (slope of 1-in-10 to 1-in-5).**

Such beach gradient values have previously been associated with shore-break waves and impact injuries in the scientific literature (Castelle *et al.*, 2019). **Given the reflective morphology type and steep gradient, shore-break impact injuries are expected to be the primary beach hazard type at Praia de Lacacao**. Rip currents are not likely to be a common beach hazard at Praia de Lacacao, as reflective beaches lack subtidal bathymetric channels that are the most common cause of rip currents (Castelle *et al.*, 2019). however, spatially variable backwash from beach cusps can result in small offshore pulses of water exiting the surf-zone known as ‘swash-rips’ (Castelle *et al.*, 2016) and these may occur at Praia de Lacacao during energetic wave conditions (i.e H_b > 1 m), but are considered by Castelle *et al.* (2016) to pose only a limited bathing hazard due to their small scale.

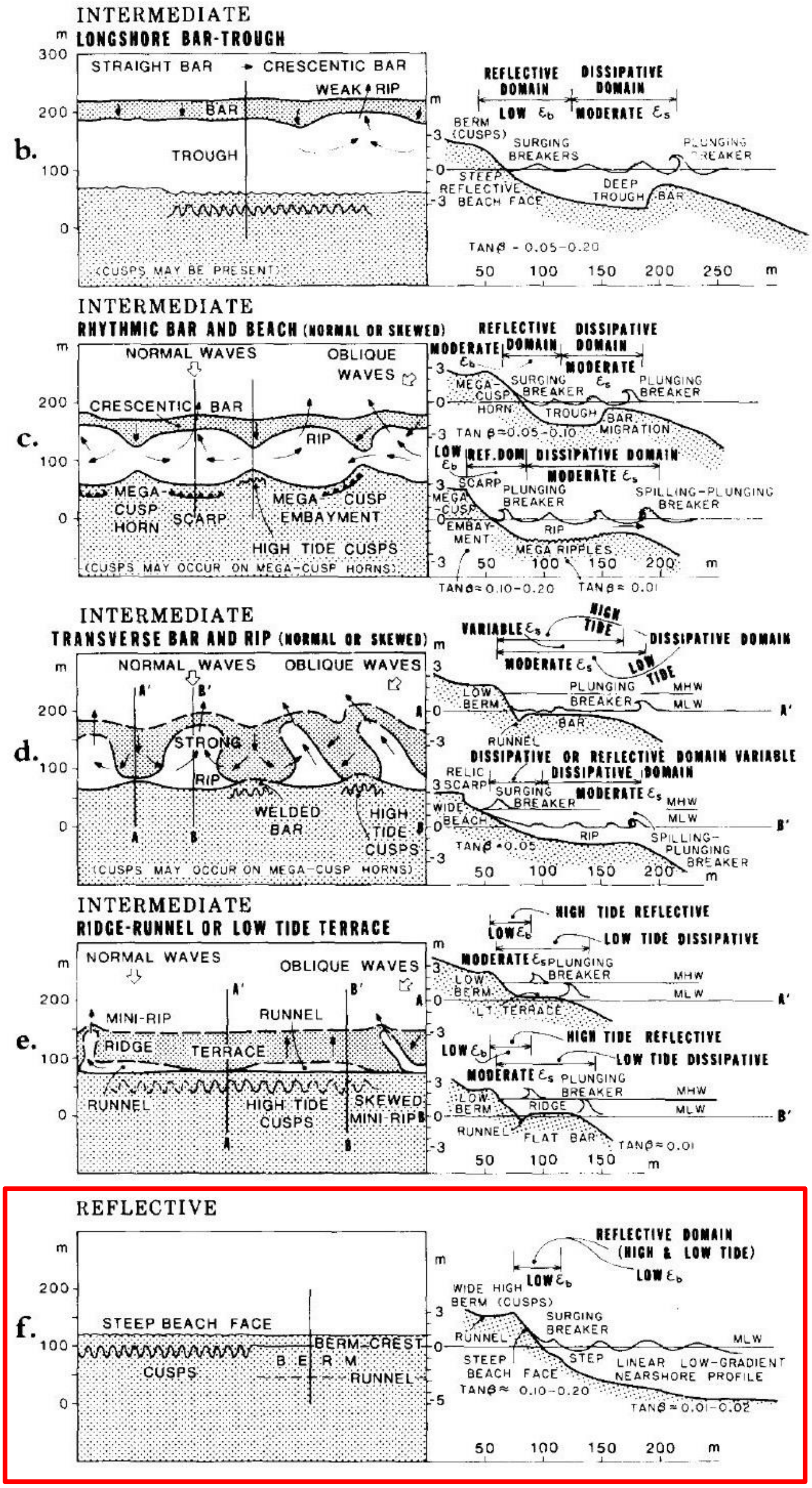

Figure 4. Beach morphology types for microtidal beaches, identified by Wright and Short (1984). The red box indicates the most likely beach morphology type to occur at Praia de Lacacao, Boa Vista, Cape Verde.

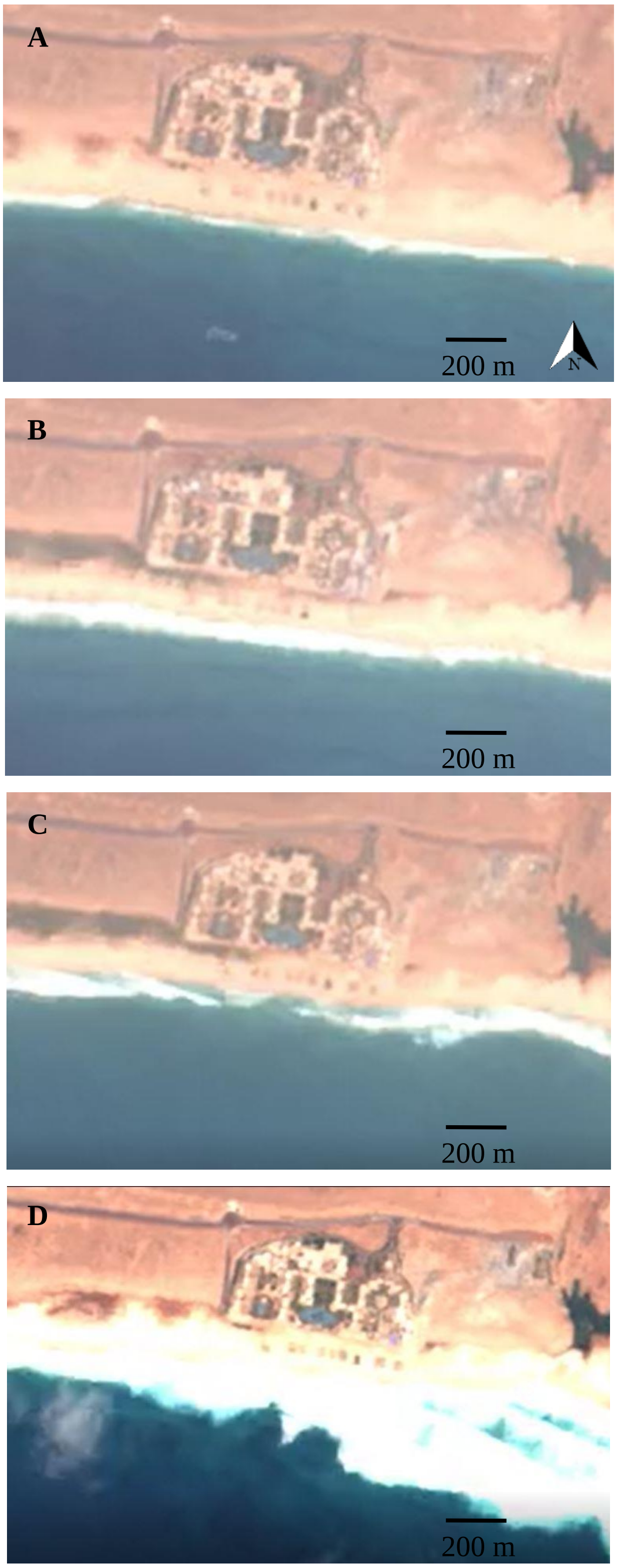

Figure 5. Sentinel-2 satellite imagery of Praia de Lacacao, Boa Vista, Cape Verde showing (from top to bottom) low to high energy wave conditions, respectively, and the full range of surf-zone width (visible as a band of white-water) from the 275 images between June 2016 and June 2020. Panel A shows typical surf-zone width, while panel D shows the widest surf-zone, which occurred only once in the images.

Figure 6. Aerial imagery of Praia de Lacacao, showing beach cusp formations at the shoreline.

Figure 7. Photograph of beach sediment at Praia de Lacacao, extracted from a tourist photograph posted on Google Maps.

3. Site Wave Climate

The most common directions from which waves arrive at Praia de Lacacao beach is from the north-east and east, driven by the north-east trade winds at this latitude; however waves also arrive less frequently from the south-east, south, and south-west (Figure 8). Waves arriving from the north will largely be blocked by the presence of Boa Vista Island itself; however, the relatively shallow coastal shelf surrounding Boa Vista (< 100 m depth; Figure 3) is expected to induce wave refraction, allowing waves from the north-east to propagate into Praia de Lacacao. Wave data for Cape Verde are extremely limited, with no historical wave buoy measurements available within or close to the island chain. Therefore, wave model data were used for the present analysis.

Wave model hindcast data were extracted from the global ocean reanalysis wave system of Météo-France (WAVERYS) with a spatial resolution of 1/5° degree (approximately 20 km), which provides global wave model data for ocean sea surface waves covering the period 15th Jan 1993 – 25th Dec 2018. These data are provided freely through the Copernicus Marine Environment Monitoring Service (CMEMS, https://marine.copernicus.eu/). Model data were extracted at a location of 15.9° latitude, -22.9° longitude (Figure 8), which is approximately 21.5 km directly offshore of Praia de Lacacao, in deep water (>1000 m depth). The wave model data for the entire hindcast period were processed and used to estimate breaking wave conditions at the beach, using the methods described in Appendix B.

Breaking waves can vary in shape and intensity between gentle ‘spilling’ breakers that dissipate their wave energy gradually over the beach profile, to ‘plunging’ breakers that break intensely over a short part of the beach profile, and finally to ‘collapsing’ or ‘surging’ breakers that dissipate their energy entirely at the shoreline. To estimate the type of wave breaking occurring at a given time (Figure 9), the Iribarren Number, ξ, was calculated (Appendix B), which is a well-established parameter used to predict the occurrence of either spilling, plunging, or surging/collapsing breakers, given information on beach slope and wave steepness (Iribarren and Nogales, 1949; Battjes, 1974). The thresholds of the Iribarren Number that differentiate different wave breaker types are shown in Table 1. Small values for ξ (i.e. $\xi < 0.4$) are attained when the beach has a gentle gradient and the incident wave field is characterized by a large wave height and a short wave length (or short wave period - the interval between each wave crest arriving at the beach). Such conditions promote the formation of gently spilling breakers. Large values of ξ (i.e. $\xi > 2$) are found when the beach is steep and the incident wave field is characterized by a small wave height and a long wave length (or long wave period). Such conditions favour the formation of surging/collapsing breakers. Plunging breakers prevail when $\xi = 0.4 – 2$.

The Iribarren Number was calculated for the entire wave hindcast period using the modelled breaking wave conditions and the upper and lower estimate of beach gradient determined in Section 2 (shallowest likely beach gradient, $\tan\beta$ = 0.1; steepest likely beach gradient, $\tan\beta$ = 0.2). Although beach slopes vary with changing wave conditions, it is expected that the beach slope at Praia de Lacacao always exists/varies somewhere within this range in the area of wave breaking, and by calculating the Iribarren Number with both the upper and lower estimate for beach slope for the entire duration of the available wave model data, the likely range and variability in wave breaker type can be assessed.

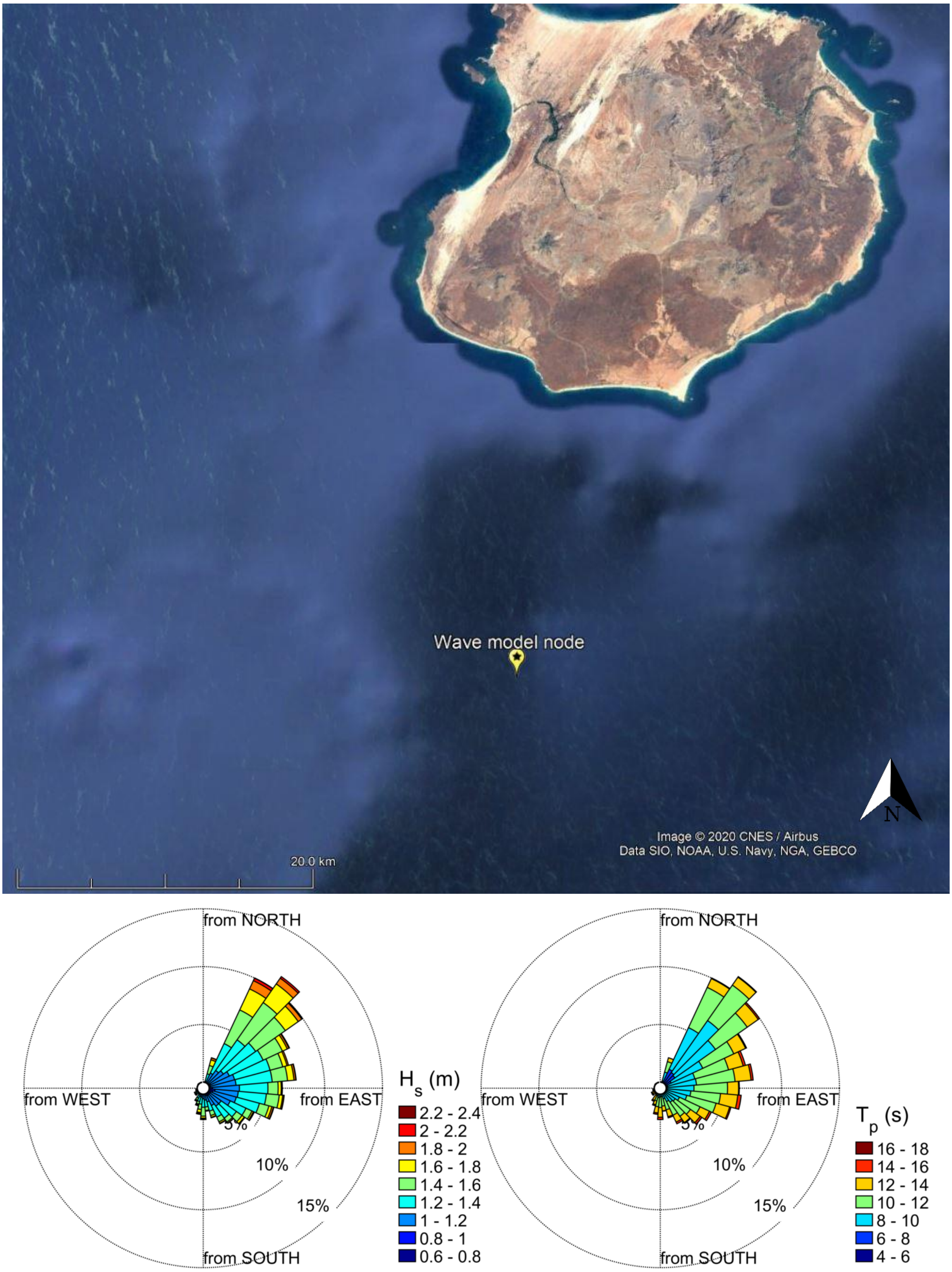

Figure 8. Upper panel: Wave model output location at 15.9° latitude, -22.9° longitude, approximately 21.5 km directly offshore of Praia de Lacacao, in deep water (>1000 m depth). Lower panels: wave roses showing proportion of wave heights (lower left) and wave periods (lower right) from different directional sectors at the wave model output location.

Table 1. Thresholds of Iribarren Number, ξ, used to differentiate between spilling, plunging, and surging/collapsing breakers

Breaker type	ξ range
Spilling	$\xi < 0.4$
Plunging	$0.4 \leq \xi \leq 2$
Surging/collapsing	$\xi > 2$

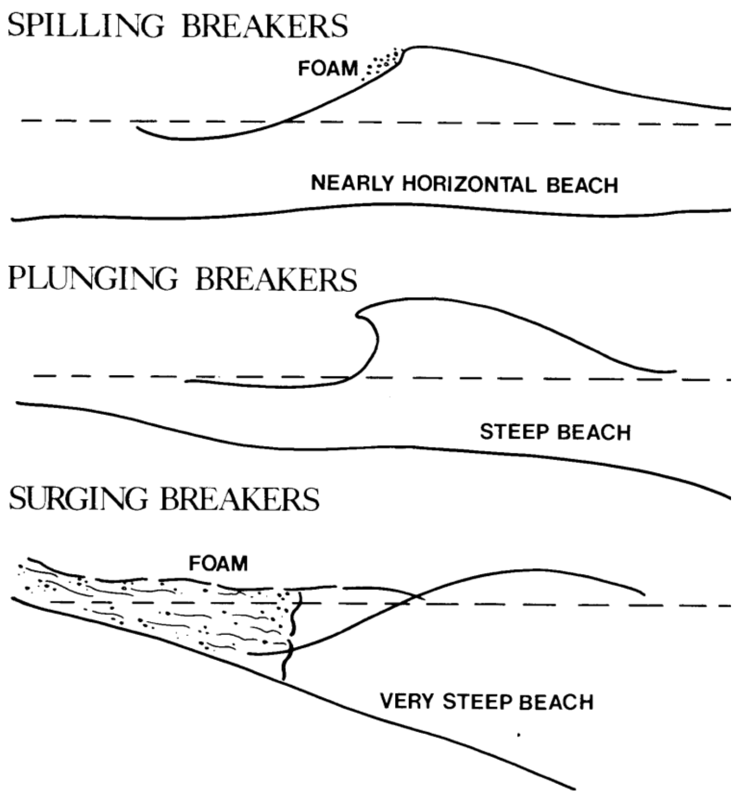

Figure 9. Cross-sectional representation of the three main types of breaking waves: spilling, plunging, surging (or collapsing).

The time-series of wave conditions at Praia de Lacacao from the WAVERYS wave model are presented in Figure 10, and are presented again in Figure 11 for the year 2012, when the bathing incidents in question occurred. Summary wave statistics are presented in Table 2 and Table 3. From the processed wave data, **breaking wave heights at the site are expected to vary from 0.5 – 3 m, but do not often exceed 1.7 m,** with only 10% of the wave data exceeding this value (Table 3). Wave conditions do not vary significantly throughout the year, and **mean summer and winter breaking wave heights vary from 0.9 – 1.0 m**, with peak wave periods of 10.2 – 11.0 s (Table 2). **Breaker type is predicted to be 'plunging' to 'surging' on average** (Table 3).

In-situ photographs of waves breaking at Praia de Lacacao at different levels of wave energy were sourced from Google Maps to verify the wave breaker types that occur at the beach. Example images are presented in Figure 12, Figure 13, and Figure 14, showing low energy (estimated as H_b < 0.5 m) to high energy (estimated as H_b > 1 m) breaking waves. These images confirm that **waves typically break very close to the beach, and under larger waves (H_b > 1m) break as plunging breakers with considerable breaking intensity and power at the shoreline.**

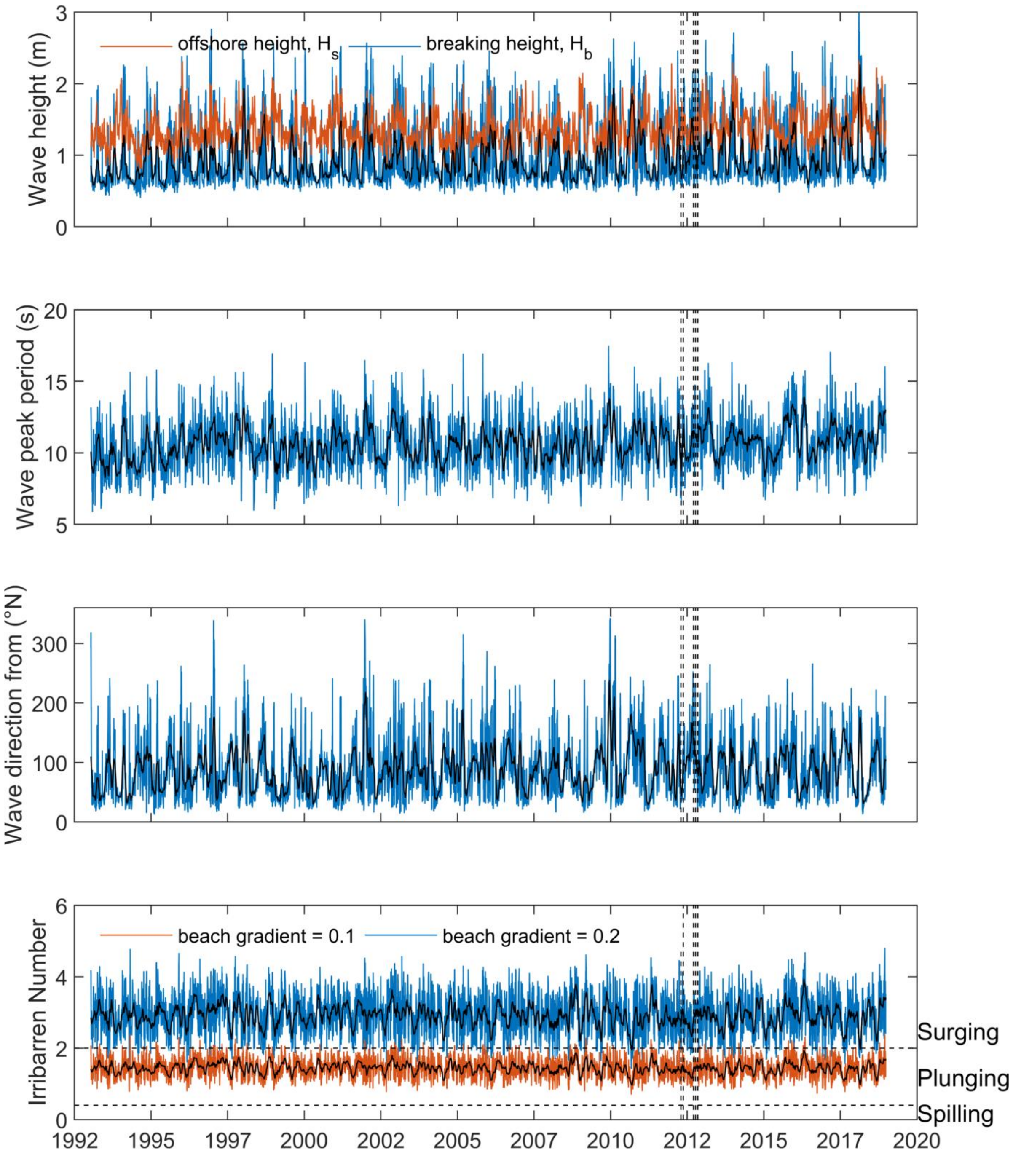

Figure 10. Wave hindcast time series from the WAVERYS global wave model, output in deep water approximately 21.5 km offshore of Praia de Lacacao. Vertical dashed lines show the dates on which the beach incidents occurred. The horizontal dashed lines in the lower panel show the thresholds that differentiate between spilling, plunging, and surging/collapsing breakers. The blue and red lines in the lower panel show the upper and lower estimate of the Iribarren Number, based on the upper and lower estimates of beach slope. Black lines in each panel show a monthly moving average (only shown for H_b in top panel for clarity).

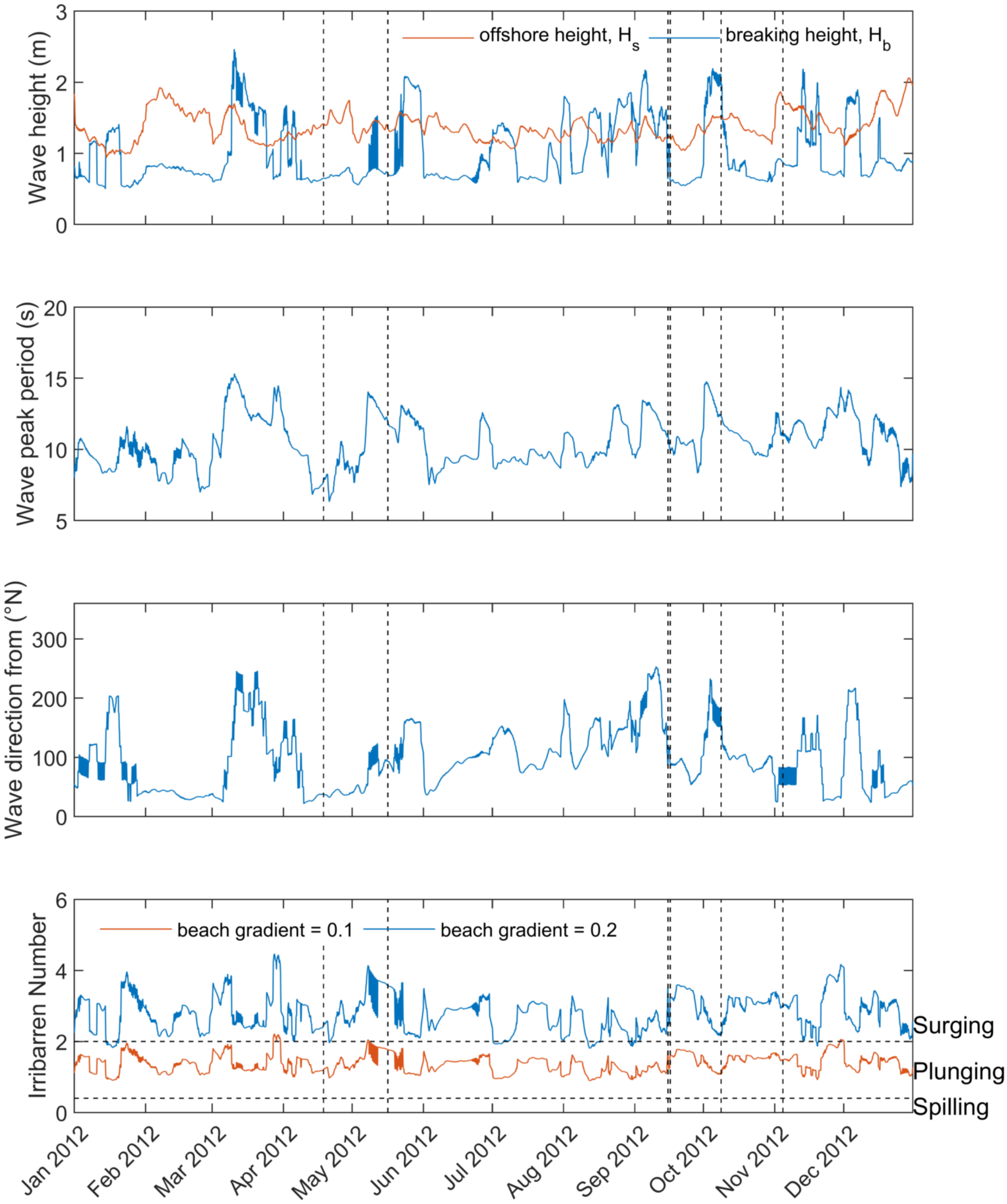

Figure 11. Wave hindcast time series from the WAVERYS global wave model, output in deep water approximately 21.5 km offshore of Praia de Lacacao, for the year 2012. Vertical dashed lines show the dates on which the beach incidents occurred. The horizontal dashed lines in the lower panel show the thresholds that differentiate between spilling, plunging, and surging/collapsing breakers. The blue and red lines in the lower panel show the upper and lower estimate of the Iribarren Number, based on the upper and lower estimates of beach slope.

Table 2. Average (mean) wave conditions at Praia de Lacacao, Boa Vista, Cape Verde, determined from the processed WAVERYS wave model data. The 'summer' averaging period was April – September, inclusive, and winter averaging period was October – March, inclusive.

Averaging period	Offshore wave height (m)	Breaking wave height (m)	Wave direction from (°N)	Wave peak period (s)	Iribarren Number ($\tan\beta$ = 0.1–0.2), breaker type	Dim. Fall velocity (ω_s= 0.25-0.5 cm/s), beach type
All	1.4	0.9	87.3	10.6	1.4–2.9, plunging - surging	0.2–0.4, reflective
Summer	1.3	0.9	87.4	10.2	1.4–2.9, plunging - surging	0.2–0.3, reflective
Winter	1.4	1.0	87.3	11.0	1.5–2.9, plunging - surging	0.2–0.4, reflective

Table 3. 10% and 90% exceedance wave conditions at Praia de Lacacao, Boa Vista, Cape Verde, determined from the processed WAVERYS wave model data.

Exceedance	Offshore wave height (m)	Breaking wave height (m)	Peak wave period (s)	Iribarren Number ($\tan\beta$ = 0.1 -0.2), breaker type	Dim. Fall velocity (ω_s= 0.25-0.5 cm/s), beach type
90%	1.1	0.6	8.4	1.1–2.2, plunging - surging	0.1–0.2, reflective
10%	1.7	1.7	12.8	1.8–3.6, plunging - surging	0.3–0.6, reflective

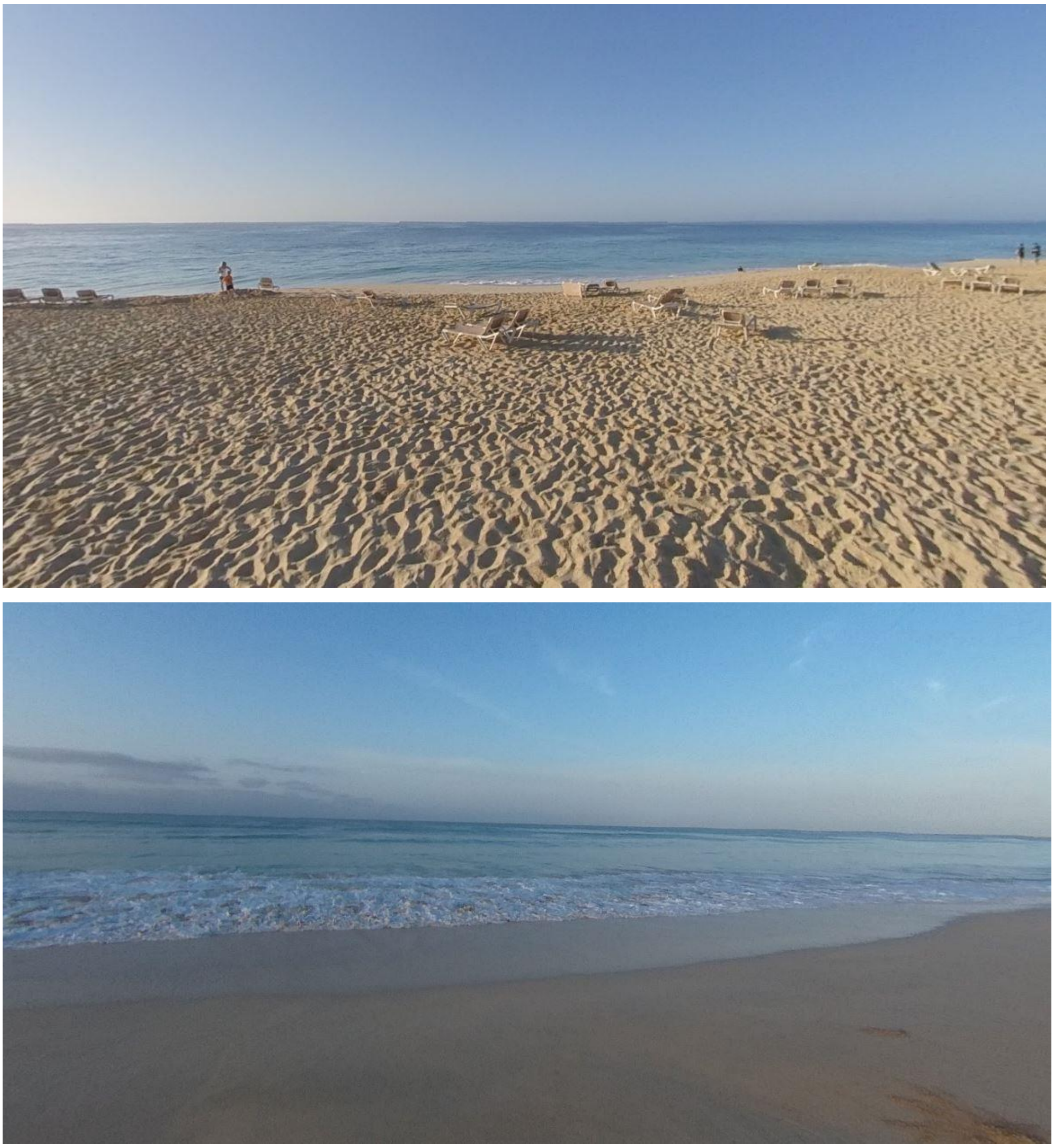

Figure 12. Examples of wave breaking at Praia de Lacacao under ‘low wave energy’ conditions (estimated as $0 < H_b < 0.5$ m).

Figure 13. Examples of wave breaking at Praia de Lacacao under ‘medium wave energy’ conditions (estimated as $0.5 < H_b < 1$ m).

Figure 14. Examples of wave breaking at Praia de Lacacao under ‘upper wave energy’ conditions (estimated as H_b >1 m).

4. Conditions at the times of the bathing incidents

From the processed wave model data, the likely wave conditions at the time of each of the bathing incidents in question can be extracted. The bathing incident wave conditions are summarised in Table 4, and time-series plots of wave conditions a week either side of each incident are presented in Figure 15 to Figure 19, Appendix C. As the wave model data has a three-hourly temporal resolution, the closest wave model prediction to the time of each incident was taken. For those incidents for which a confirmed time was not provided (Table 4), the time was assumed to be 12:00 (midday) for the purposes of this analysis.

During incidents 1, 2, 3, 4, and 6 (Table 4), the wave conditions are predicted to have been below the average breaking wave height for the season in which they occurred (Table 2), ranging from H_b = 0.6 m – 0.9 m. Waves during these incidents are predicted to have been arriving from the east and north-east directions and would have lost some energy due to refraction before arriving at Praia de Lacacao. **During incident 5 (Table 4), the wave conditions are predicted to have been H_b = 2 m – a wave height which is exceeded less than 10% of the time at Praia de Lacacao (Table 3)**. The waves during incident 5 are predicted to have arrived from the south-east direction, and therefore would have undergone less refraction and energy loss than the waves during the other incidents. **During all of the incidents, plunging to surging breakers are predicted to have been occurring on the beach (Table 4).**

Table 4. Predicted wave conditions at Praia de Lacacao, Boa Vista, Cape Verde at the times of the bathing incidents, determined from the processed WAVERYS wave model data.

Incident No.	Incident Date	Offshore wave height (m)	Breaking wave height (m)	Wave direction from (°N)	Peak wave period (s)	Iribarren Number ($\tan\beta =$ 0.1–0.2), breaker type
1	18th April 2012, time unconfirmed	1.4	0.7	38	7.8	1.2–2.5, plunging - surging
2	16 May 2012, 12:00	1.4	0.7	94	11.9	1.8–3.6, plunging - surging
3	15 September 2012, time unconfirmed	1.2	0.6	85	11.0	1.7–3.5, plunging - surging
4	16 September 2012, time unconfirmed	1.2	0.6	90	10.0	1.6–3.2, plunging - surging
5	8 October 2012, 15:00	1.5	2.0	152	12.3	1.1–2.2, plunging - surging
6	4 November 2012, 13:00	1.8	0.9	82	11.0	1.5–3.0, plunging - surging

5. Conclusions

- Through a process of expert judgement using a combination of wave analysis, and assessment of in-situ and satellite imagery, the beach at Praia de Lacacao is expected to be consistently at the ‘reflective’ end of the beach morphology spectrum. The likely beach profile gradient in the area of wave breaking is expected to be consistently within the range 0.1 – 0.2 (slope of 1-in-10 to 1-in-5), which represents a steep beach profile.
- Given the reflective morphology type and steep gradient, shore-break impact injuries are expected to be the primary beach hazard type at Praia de Lacacao.
- From processed wave model data, breaking wave heights at the site are predicted to vary from 0.5 – 3 m, but only exceed 1.7 m 10% of the time.
- Wave conditions do not vary significantly throughout the year, and average summer and winter breaking wave heights vary from 0.9 – 1.0 m, with peak wave periods of 10.2 – 11.0 s.
- Wave breaking is predicted to be consistently within the ‘plunging’ to ‘surging’ regimes.
- In-situ photographs of waves breaking at Praia de Lacacao confirm that waves typically break very close to the beach, and under larger waves (H_b > 1 m) break as plunging breakers with considerable breaking intensity and power at the shoreline.
- During five of the six bathing incidents, the wave conditions are predicted to have been below the average breaking wave height for the season in which they occurred, ranging from H_b = 0.6 m – 0.9 m.
- During one of the six incidents, the wave conditions are predicted to have been H_b = 2 m – a wave height which is exceeded less than 10% of the time at Praia de Lacacao.
- During all of the incidents, plunging to surging breakers are predicted to have been occurring on the beach.

References

Baldock, T. E., Holmes, P., Bunker, S. and Van Weert, P. 1998. Cross-shore hydrodynamics within an unsaturated surf zone. *Coastal Engineering*, **34**, (3-4), 173-196.

Battjes, J. A. 1974. *Surf similarity*. 14th International Conference on Coastal Engineering. Copenhagen.

Castelle, B., Scott, T., Brander, R., McCarroll, J., Robinet, A., Tellier, E., Korte, E. d., Simonnet, B. and Salmi, L.-R. 2019. Environmental controls on surf zone injuries on high-energy beaches. *Natural Hazards and Earth System Sciences*, **19**, (10), 2183-2205.

Castelle, B., Scott, T., Brander, R. W. and McCarroll, R. J. 2016. Rip current types, circulation and hazard. *Earth-Science Reviews*, **163**, 1-21.

Dean, R. G. 1991. Equilibrium beach profiles: characteristics and applications. *Journal of Coastal Research*, **7**, 53-84.

Iribarren, C. and Nogales, C. 1949. Protection des Ports. XVIIth International Navigation Congress. Section II, Communication. **4**4)

Masselink, G. and Short, A. D. 1993. The effect of tide range on beach morphodynamics and morphology: a conceptual beach model. *Journal of Coastal Research*, **9**, 785-800.

van Rijn, L. C. 2014. A simple general expression for longshore transport of sand, gravel and shingle. *Coastal Engineering*, **90**, 23-39.

Wright, L. D. and Short, A. D. 1984. Morphodynamic variability of surf zones and beaches: A synthesis. *Marine Geology*, **56**, 93-118.

Appendix A. Expertise of the CMAR team

CMAR is the commercial consultancy arm of the Coastal Processes Research Group (CPRG) at the University of Plymouth, UK. Over the last 10 years, CPRG's research and consultancy work has significantly impacted beach lifeguarding risk assessment, training and policy in the UK, South Africa and New Zealand. CPRG's rip current forecasts are used in the UK and NZ, informing daily lifeguard resourcing. CPRG's expertise informed coroners' drowning inquiries in the UK and SA, and directly led to changes in risk management policy at two UK beaches and one beach in SA. The research underpins annual RNLI risk assessments at all UK bathing waters and annual lifeguard training material, and has informed rip current safety advice globally.

The team assembled for this project consist of **Professor Gerd Masselink** (director of CMAR), **Dr Tim Scott** (project lead), and **Dr Christopher Stokes** (lead consultant). **Gerd Masselink** is a Professor in Coastal Geomorphology with over 20 years' experience in collecting and analysing coastal data, and over 100 papers published in peer-reviewed international journals. Prof. Masselink published one of the most widely used beach morphology classification models and is an international expert on beach morphodynamics. **Dr Tim Scott** is a lecturer in Ocean Exploration and has been actively contributing to internationally recognised research in fields of beach and submarine geomorphology, rip current dynamics and coastal hazards. He has undertaken doctoral and post-doctoral research projects into physical beach hazards, and is an international expert on beach morphology, rip current dynamics, and physical beach hazards. **Dr Christopher Stokes** is a senior research consultant and has undertaken three consultancy projects for the RNLI mapping out which beaches in the UK pose the greatest life-risk to bathers, and has published research on modelling beach-user numbers and beach life-risk.

The team have collectively undertaken the following research and consultancy projects related to beach hazards:

- 2020–present, Newton Fund: Weather and Climate Science Services Partnership (WCSSP) SA: Marine and Coastal Applications. C Stokes: research consultant; T Scott: co-investigator; G Masselink: project lead. £80,000.
- 2018–2019, Auckland Council/Surf Life Saving Northern Regions: Safeswim Beach Risk Forecasting. C Stokes: research consultant; T Scott: co-investigator; G Masselink: project lead. £76,000.
- 2015–2018, RNLI: Quantification of Beach Risk in the UK and Northern Ireland. C Stokes: research consultant; T Scott: co-investigator; G Masselink: project lead. £105,000.
- 2012–2014, RNLI/MetOffice/Marine Institute: Topographic rip currents TOPORIP. T Scott: co-investigator. £99,000.

- 2010–2014, NERC/RNLI – Partnership grant: Dynamics of Rips and Implications for Beach Safety. T Scott: research fellow; G. Masselink: primary investigator. £550,000.
- 2009, RNLI: UK beach and hazards database project: Good Beach Guide integration. T Scott: primary investigator. £10,000.
- 2006–2008, RNLI: Classification and risk assessment of UK beaches. G Masselink: co-investigator. £30,000.

Below is a sample of some of the relevant research articles that the team have published in leading international peer-reviewed science journals:

- Castelle B, **Scott T**, Brander R, McCarroll RJ, Tellier E, de Korte E, Tackuy L, Robinet A, Simonnet B & Salmi L-R 2020 'Wave and Tide Controls on Rip Current Activity and Drowning Incidents in Southwest France' Journal of Coastal Research 95, (sp1) 769-769.
- Castelle B, **Scott T**, Brander R, McCarroll J, Robinet A, Tellier E, de Korte E, Simonnet B & Salmi L-R 2019 'Environmental controls on surf zone injuries on high-energy beaches' Natural Hazards and Earth System Sciences 19, (10) 2183-2205.
- **Scott T**, Castelle B, Almar R, Senechal N, Floc'h F & Detandt G 2018 'Controls on Flash Rip Current Hazard on Low-Tide Terraced Tropical Beaches in West Africa' Journal of Coastal Research 92-99.
- Castelle B, Brander R, Tellier E, Simonnet B, **Scott T**, McCarroll J, Campagne J-M, Cavailhes T & Lechevrel P 2018 'Surf zone hazards and injuries on beaches in SW France' Natural Hazards.
- **Stokes, C., Masselink, G**., Revie, M., **Scott, T**., Purves, D. and Walters, T., 2017. Application of multiple linear regression and Bayesian belief network approaches to model life risk to beach users in the UK. Ocean & Coastal Management, 139, pp.12-23.
- Castelle B, **Scott T**, Brander RW & McCarroll RJ 2016 'Rip current types, circulation and hazard' Earth-Science Reviews 163, 1-21
- **Scott T**, Austin M, **Masselink G** & Russell P 2016 'Dynamics of rip currents associated with groynes — field measurements, modelling and implications for beach safety' Coastal Engineering 107, 53-69.
- **Scott T, Masselink G**, Austin MJ & Russell P 2014 'Controls on macrotidal rip current circulation and hazard' GEOMORPHOLOGY 214, 198-215
- Austin MJ, **Masselink G**, **Scott TM** & Russell PE 2014 'Water-level controls on macro-tidal rip currents' Continental Shelf Research 75, 28-40.

- Austin, M.J., **Scott, T.M**., Russell, P.E. and **Masselink, G**., 2013. Rip current prediction: development, validation, and evaluation of an operational tool. Journal of coastal research, 29(2), pp.283-300.
- **Scott T, Masselink G** & Russell P 2011 'Morphodynamic characteristics and classification of beaches in England and Wales' MARINE GEOLOGY 286, (1-4) 1-20.
- Austin M, **Scott T**, Brown J, Brown J, MacMahan J, **Masselink G** & Russell P 2010 'Temporal observations of rip current circulation on a macro-tidal beach' Continental Shelf Research 30, (9) 1149-1165.
- **Scott T**, Russell P, **Masselink G**, Wooler A & Short A 2007 'Beach Rescue Statistics and their Relation to Nearshore Morphology and Hazards: A Case Study for Southwest England' J COASTAL RES (SI 50) 1-6.
- **Masselink G** & Short A 1993 'The effect of tide range on beach morphodynamics and morphology - a conceptual beach model' Journal of Coastal Research 9, (3) 785-800.

Appendix B. Processing of wave model data

From the offshore wave model data, breaking wave height at the beach was calculated using an empirical equation (van Rijn, 2014) that estimates breaking wave height, water depth and direction using linear wave theory and Snell's law for refraction:

$$h_b = \left[\left(H_{s,o}{}^2 C_o \cos\theta_o\right)/(1.8\,\gamma^2 g^{0.5})\right]^{0.4} \tag{1}$$

and

$$\sin\theta_b = (C_b/C_o)\sin\theta_o \tag{2}$$

where h_b = the water depth at the breaker line, $H_{s,o}$ = the offshore significant wave height output by the wave model, C_o, C_b = the offshore and breaking wave propagation speeds, and θ_o, θ_b = the offshore and breaking wave incidence angles relative to shore normal (for Praia de Lacacao, shore normal = 185°). Snell's law for refraction is limited to waves arriving from a direction within 90° of shore-normal, and therefore all waves were assumed to arrive at Praia de Lacacao within this directional window. C_o was calculated from the deepwater wavelength, L_o, and peak wave period, T_p, as $C_o = L_o/T_p$, while C_b was calculated as $C_b = \sqrt{gh_b}$. Breaker criterion γ is a key parameter that determines the depth at which wave breaking occurs, and was defined using the offshore wave steepness, $S_0 = H_{rms,0}/L_0$, where $H_{rms,0}$ is the deep water root-mean-square wave height, following Baldock *et al.* (1998) as:

$$\gamma = 0.39 + 0.56\tanh(33S_0) \tag{3}$$

The breaking wave height can then be calculated as the product of the breaker criterion and breaker depth:

$$H_b = \gamma h_b \tag{4}$$

The Iribarren Number was calculated from the breaking wave height, deepwater wavelength and estimated beach slope ($\tan\beta$) as (Battjes, 1974):

$$\varepsilon = \frac{\tan\beta}{\sqrt{H_b/L_0}} \tag{5}$$

Appendix C. Wave conditions for each incident

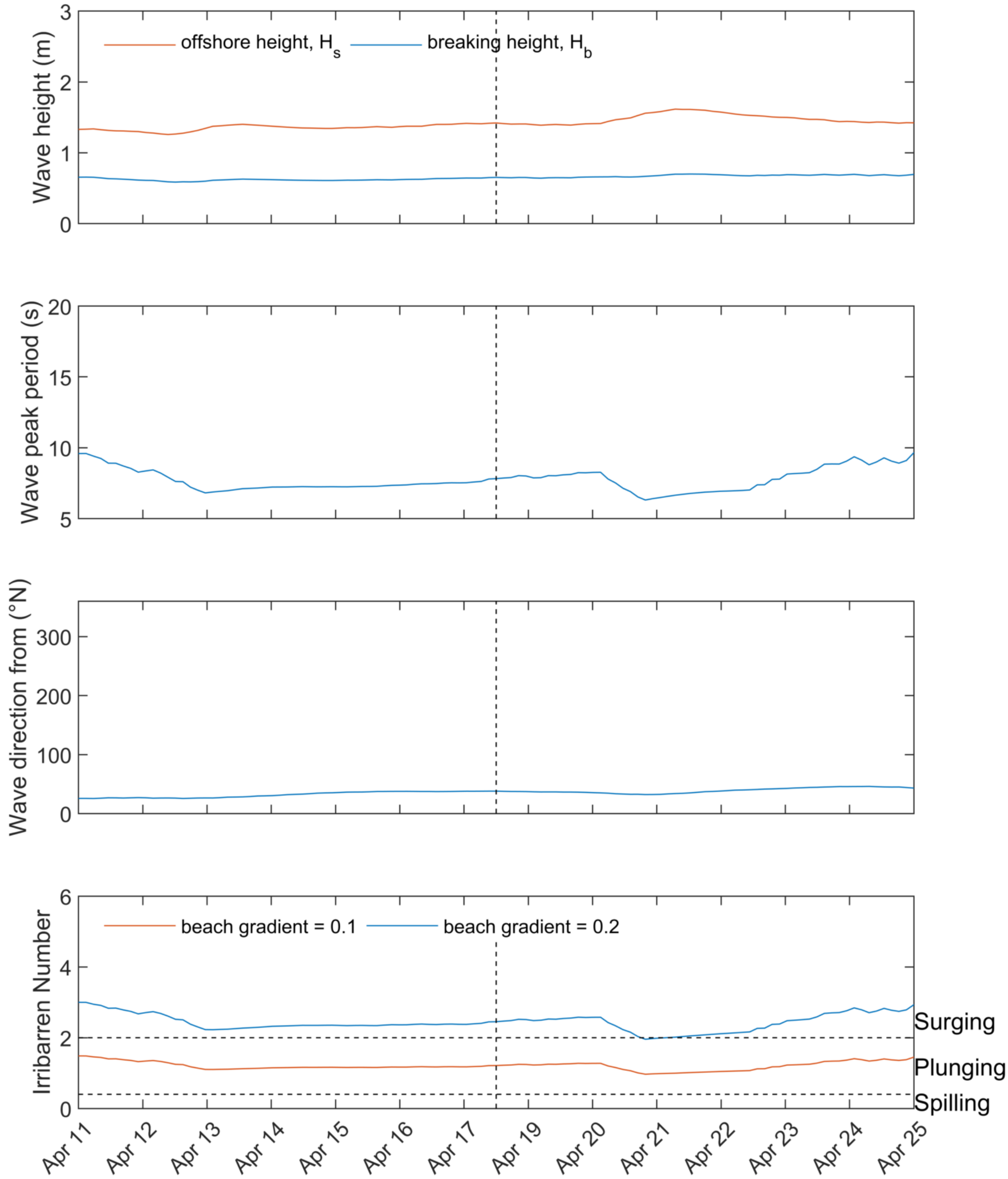

Figure 15. Wave conditions for a week either side of incident number 1 (18th April 2012).

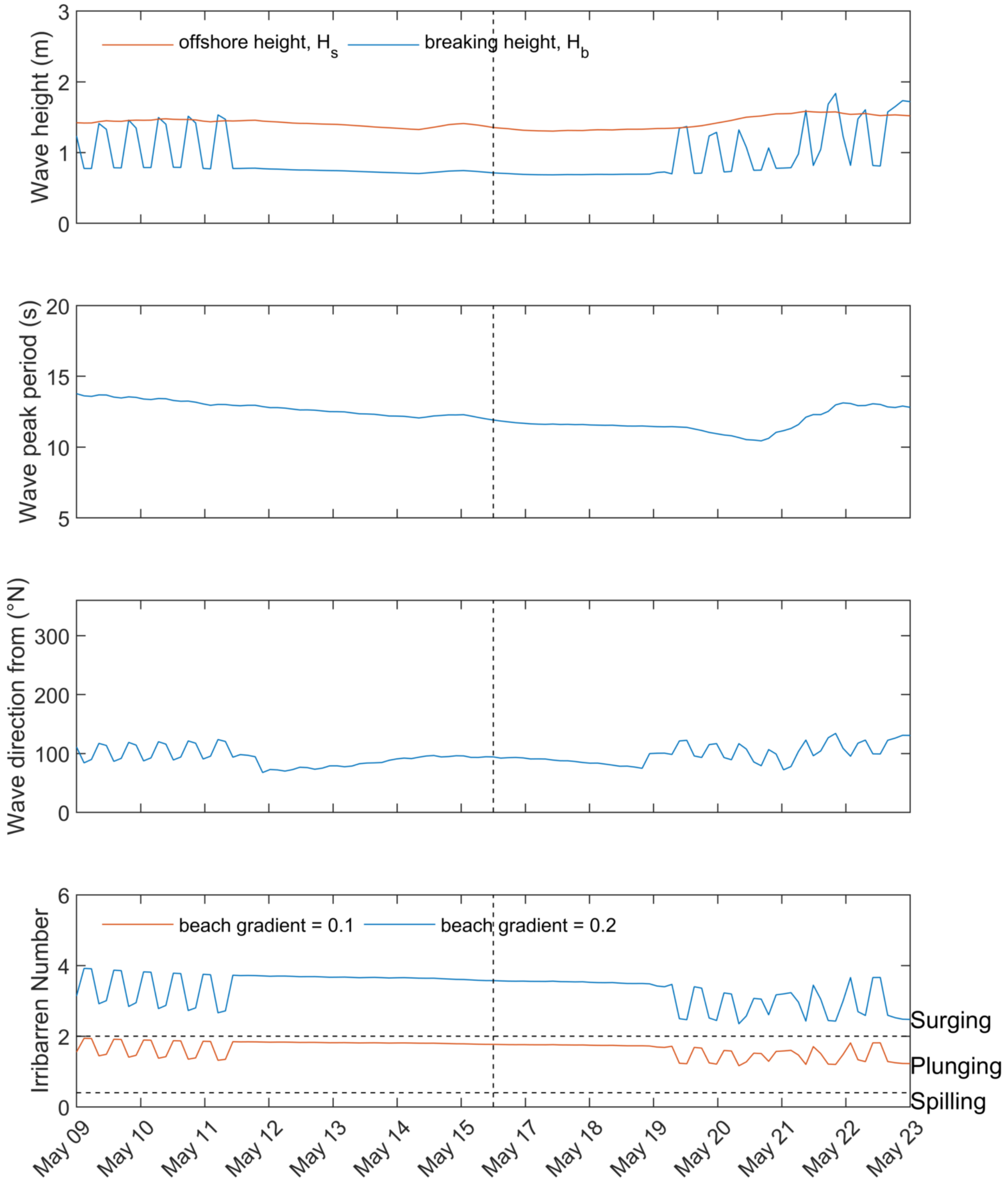

Figure 16. Wave conditions for a week either side of incident number 2 (16th May 2012).

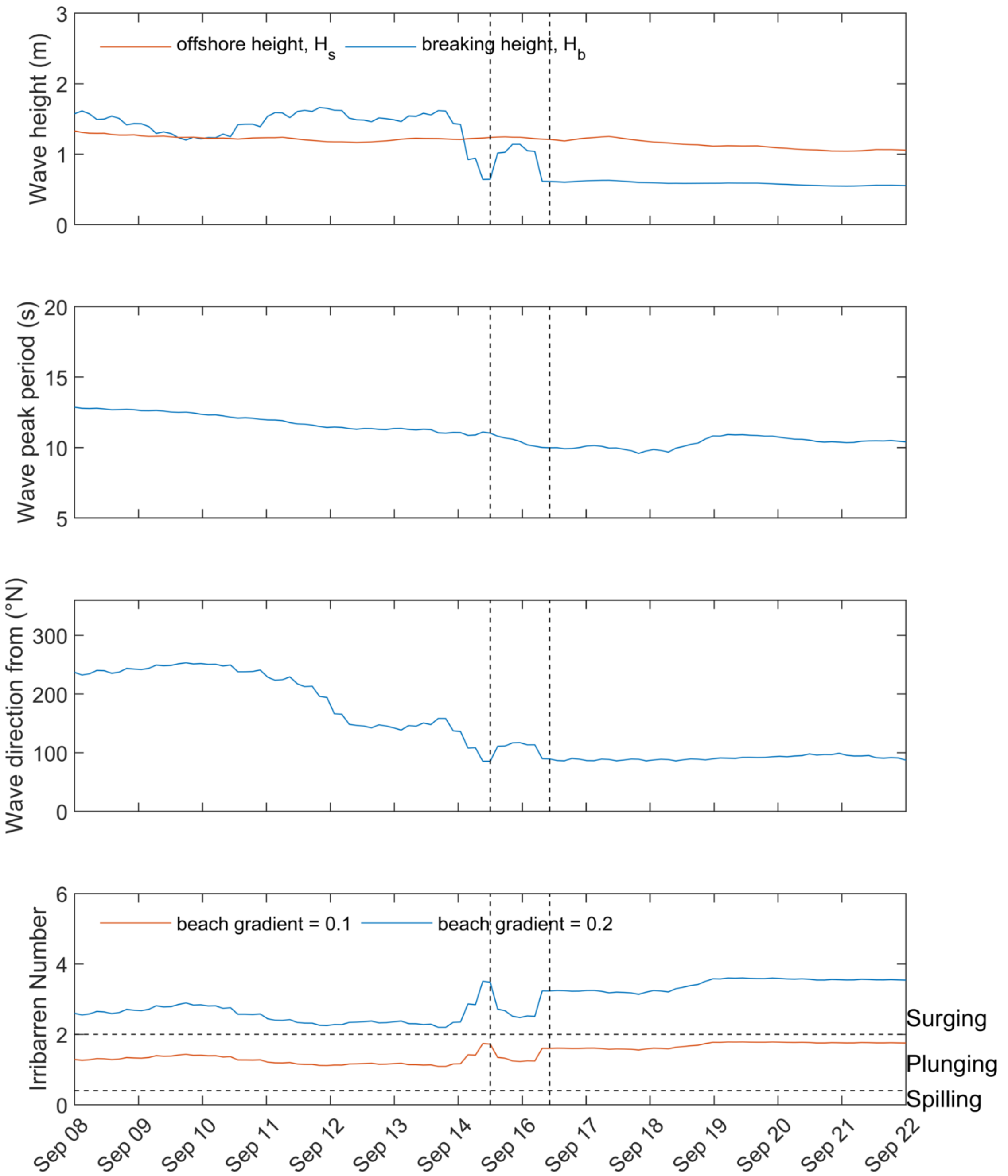

Figure 17. Wave conditions for a week either side of incident number 3 and 4 (15th and 16th of September 2012).

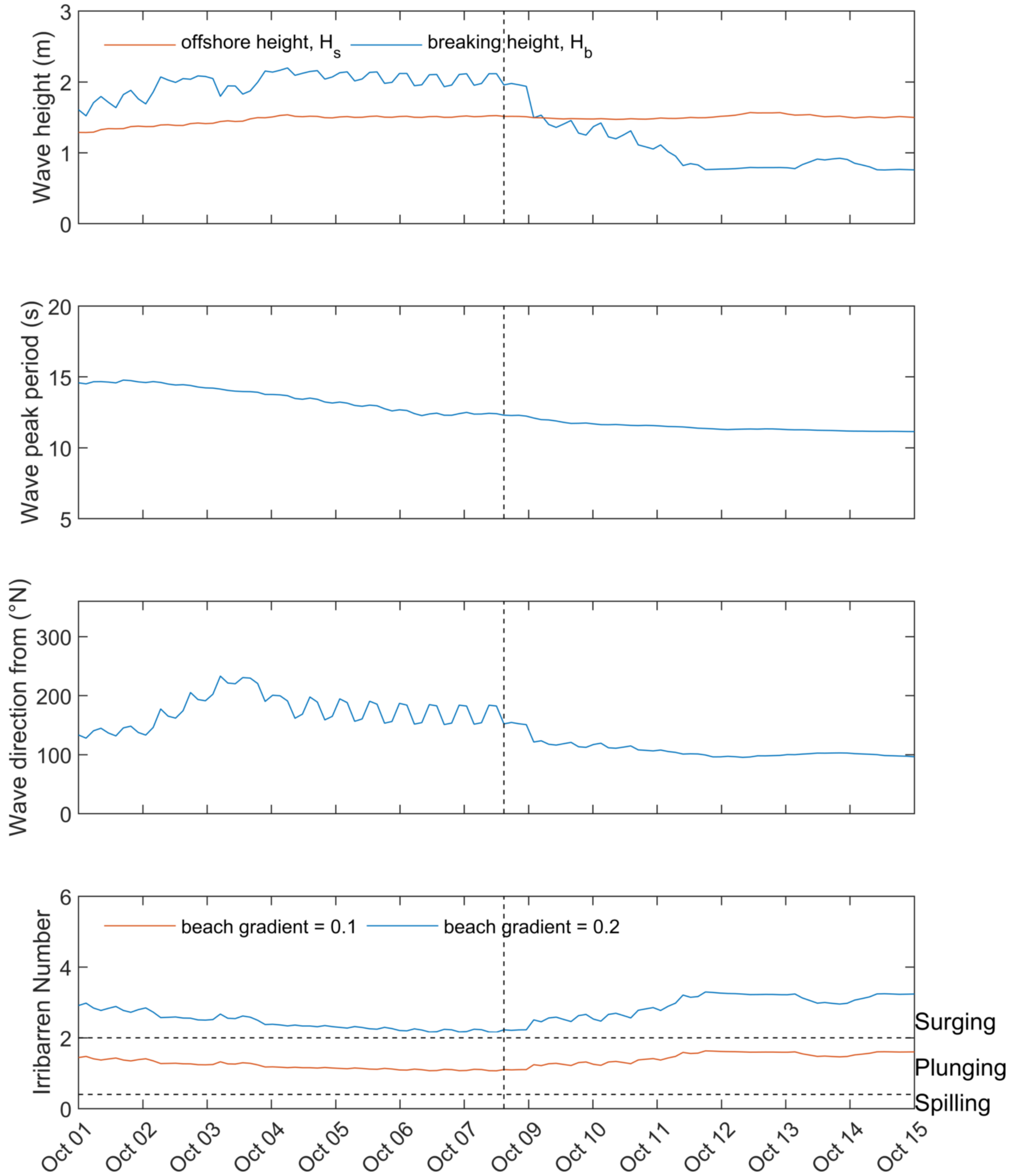

Figure 18. Wave conditions for a week either side of incident number 5 (8th October 2012).

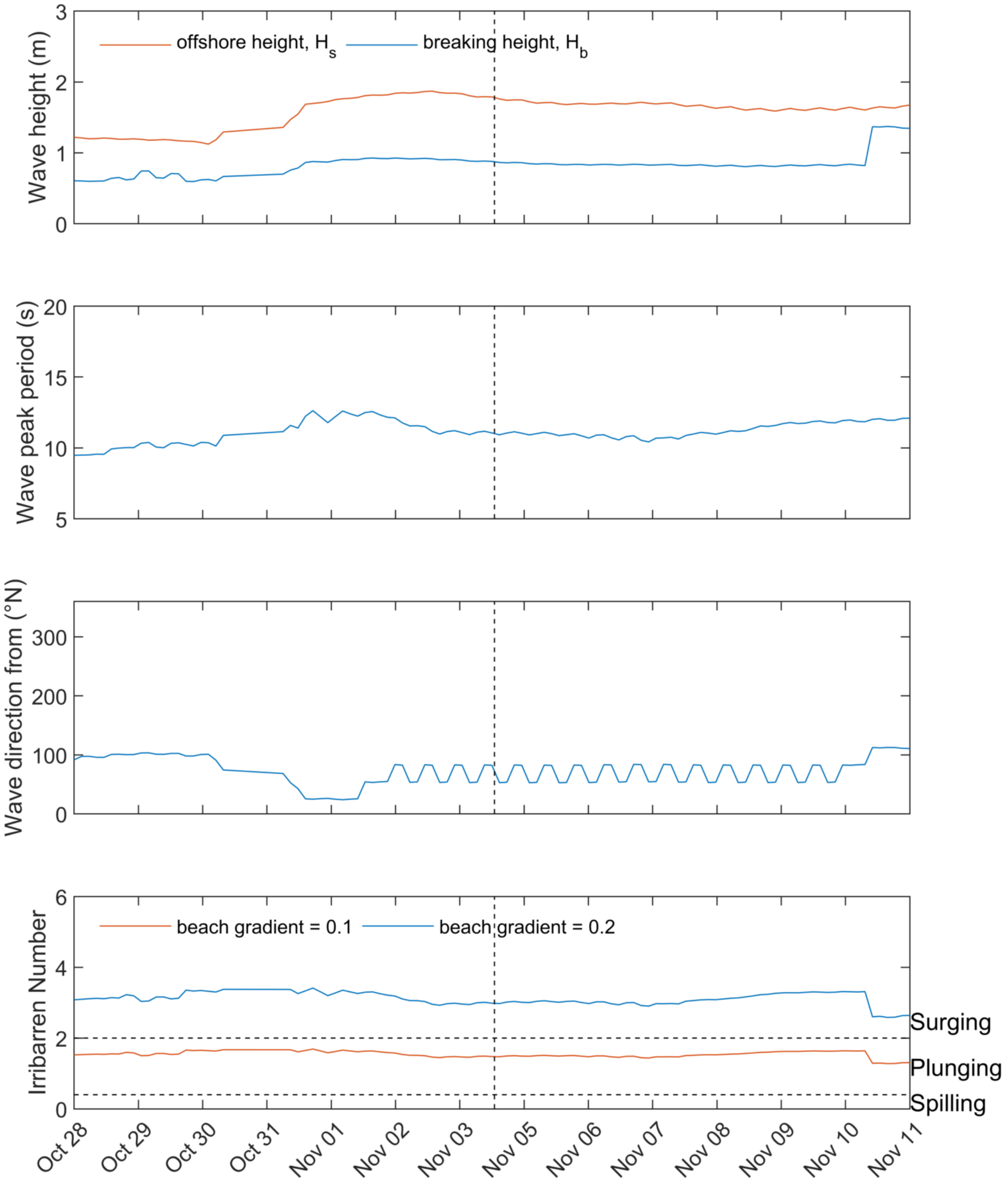

Figure 19. Wave conditions for a week either side of incident number 6 (4th November 2012).